Interlayer Exchange Coupling: A General Scheme Turning Chiral Magnets into Magnetic Multilayers Carrying Atomic-Scale Skyrmions

Ashis Kumar Nandy,* Nikolai S. Kiselev, and Stefan Blügel
Peter Grünberg Institut and Institute for Advanced Simulation, Forschungszentrum Jülich and JARA, D-52425 Jülich, Germany
(Received 28 September 2015; revised manuscript received 4 March 2016; published 28 April 2016)

We report on a general principle using interlayer exchange coupling to extend the regime of chiral magnetic films in which stable or metastable magnetic Skyrmions can appear at a zero magnetic field. We verify this concept on the basis of a first-principles model for a Mn monolayer on a W(001) substrate, a prototype chiral magnet for which the atomic-scale magnetic texture is determined by the frustration of exchange interactions, impossible to unwind by laboratory magnetic fields. By means of *ab initio* calculations for the $Mn/W_m/Co_n/Pt/W(001)$ multilayer system we show that for certain thicknesses m of the W spacer and n of the Co reference layer, the effective field of the reference layer fully substitutes the required magnetic field for Skyrmion formation.

DOI: 10.1103/PhysRevLett.116.177202

Chiral magnetic Skyrmions are localized magnetic vortices with particlelike properties. They may occur as stable or metastable states in chiral magnets due to the competition between Heisenberg exchange and the Dzyaloshinskii-Moriya interaction (DMI) [1,2], which is the essential ingredient for Skyrmion stabilization. The unique static and dynamic properties of magnetic Skyrmions driven by their nontrivial topology make them attractive for practical application in spintronic devices [3,4] and interesting objects for fundamental research.

The DMI is the result of the spin-orbit coupling (SOC) that occurs in magnetic systems with broken inversion symmetry. The systems where chiral Skyrmions have been observed so far can be divided into three main classes: (i) noncentrosymmetric bulk crystals, e.g., MnSi [5], FeGe [6], FeCoSi [7], (ii) thin films of noncentrosymmetric crystals e.g., MnSi [8], FeGe [9], FeCoSi [10], and (iii) ultrathin layers and multilayers with a surface or interface induced DMI [11–13]. The latter class of materials seems very promising, because it is most compatible with device technology, and varying the thickness of the layers and the composition at the interface allows us to tune intrinsic parameters such as the exchange, DMI, magnetic anisotropy, etc., in a wide range [13–15].

Of particular interest are atomic-scale isolated Skyrmions (iSks), whose stability is robust over a large range of magnetic fields and temperatures. This brings into play ultrathin layers of chiral magnets with nonmicromagnetically describable magnetic behavior due to the competing ferro- and antiferromagnetically coupled exchange interactions between different atomic sites that are finally the origin of stable achiral exchange spin spirals (SSs) of atomic length scale. In this case, the role of the DMI is to select a particular chirality of the spirals. From micromagnetic theory [16,17] it is known that for a given spin stiffness, DMI, and anisotropy, there is in principle always a range of applied magnetic fields that lead to the Skyrmion phase. We show that ultrathin films of chiral magnets with exchange driven SSs possess the same properties as conventional chiral magnets, but the energy scale translates into gigantic magnetic fields that are not accessible in the laboratory, and thus those types of magnets had been excluded so far. A prototype system for this type of magnet is a monolayer (ML) of Mn on a W(001) substrate with an experimentally confirmed [18] atomic-scale chiral exchange stabilized SS, but no Skyrmions could be found.

In this Letter, we propose interlayer exchange coupling (IEC) [19–22] as an elegant approach to stabilize Skyrmions without an external field and thus to widen the class of chiral magnets hosting Skyrmions. We justify our concept by calculations within a multiscale model based on *ab initio* calculations and atomistic simulations in the frame of a classical spin model. The model put forward applies to ultrathin transition-metal films deposited on a nonmagnetic heavy metal substrate where the DMI is induced by the interface due to the strong SOC [23]. In such a system, the Skyrmions may appear under a magnetic field applied perpendicular to the layer, Fig. 1(a). Alternatively, we propose that the Skyrmion phase can be stabilized by designing multilayers composed of two magnetic layers (top free and bottom reference layers) separated by a nonmagnetic spacer layer, where the applied magnetic field is substituted by the IEC, which acts as an effective magnetic field, see Fig. 1(b). In this approach, the system should satisfy the following conditions: (i) the reference layer should be a hard ferromagnet with a large exchange stiffness and a strong out-of-plane anisotropy, (ii) the effective field induced by the IEC should be in the range of the magnetic field required for Skyrmion stabilization, and (iii) the internal properties, mainly the exchange coupling and the strength of the DMI of the free layer, remain nearly the same as in the parent system.

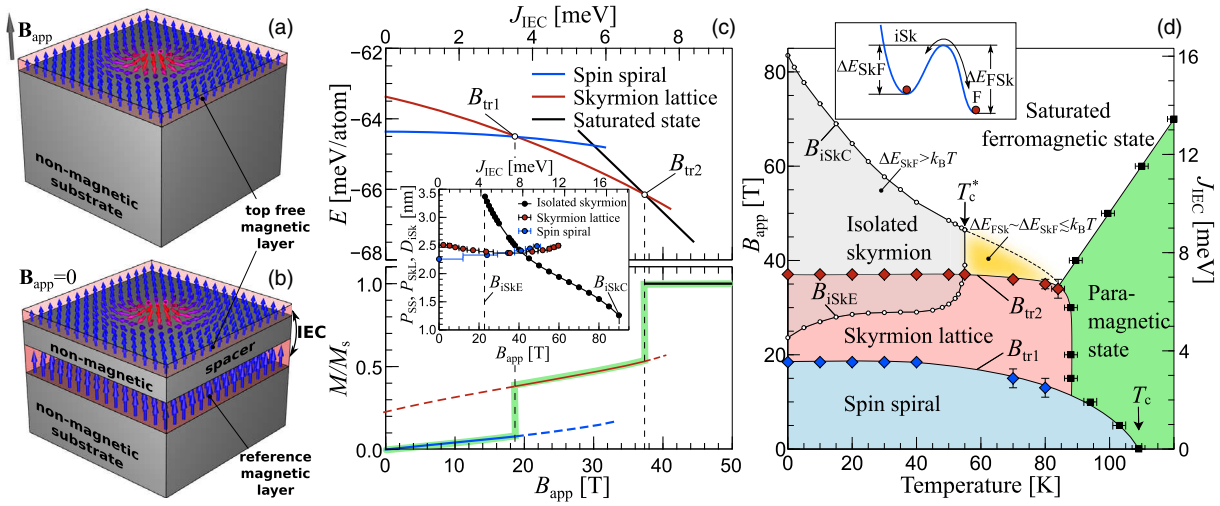

FIG. 1. Schematic representation of (a) the single magnetic layer system with Skyrmions stabilized by a magnetic field, B_{app}, applied normally to the film and (b) an equivalent multilayer system with B_{app} replaced by the IEC between the top free and underlying reference magnetic layers with a fixed out-of-plane magnetization. (c) Energy density (top panel) and average out-of-plane magnetization (bottom panel) for a SS, hexagonal SkL, and saturated FM state as functions of B_{app} (bottom axis) as well as the corresponding J_{IEC} (top axis) calculated for Mn/W(001) at zero temperature. The solid green line corresponds to the equilibrium magnetization; the dashed lines correspond to metastable states. The inset shows the dependence of the equilibrium period length P of the SS and the hexagonal SkL, and the size of the isolated Skyrmion (iSk) as a function of B_{app} and J_{IEC}. (d) Magnetic phase diagram for Mn/W(001). The SkL is energetically most favorable in the range between B_{tr1} and B_{tr2} (red area). The range of existence for the iSk (shaded gray area) is bounded by an elliptical instability field B_{iSkE} and a collapse field B_{iSkC} and intersects with the range of the equilibrium SkL. The temperature stability of the iSks is restricted by the critical temperature T_c^*, above which the iSks appear in the Skyrmion soup state (yellow area) where Skyrmions with a short lifetime exhibit spontaneous annihilation and nucleation. In the inset, ΔE_{SkF} and ΔE_{FSk} define the energy barriers for the transition from the iSk state to the FM state and the reverse one, respectively. For details see Ref. [24].

To describe such a multilayer system we use the following model Hamiltonian, comprising the contribution from the Heisenberg exchange, the DMI, the out-of-plane anisotropy, the Zeeman interaction, and IEC between the free and reference layers:

$$\mathcal{H} = -\sum_{i<j} J_{ij}(\hat{m}_i \cdot \hat{m}_j) - \sum_{\langle i<j\rangle} \vec{D}_{ij} \cdot [\hat{m}_i \times \hat{m}_j] - \sum_i K(m_i^z)^2 - \sum_i \mu \vec{B}_{\mathrm{app}} \cdot \hat{m}_i - \sum_{\langle i<j\rangle} J_{\mathrm{IEC}}(\hat{m}_i \cdot \hat{m}_{Rj}), \quad (1)$$

where $\langle i<j\rangle$ denotes a summation over all the nearest-neighbor pairs. $\hat{m}$ and $\hat{m}_R$ are the unit vectors of the magnetic moment in the free and reference layers, respectively, and μ is the absolute value of the magnetic moment of a free layer atom. For a fixed magnetization in the hard reference layer, $\vec{m}_{Ri} = \vec{m}_R$ for all sites i; the IEC term $\mathcal{H}_{\mathrm{IEC}}$ can be rewritten as $\mathcal{H}_{\mathrm{IEC}} = -\sum_i \mu \vec{B}_{\mathrm{eff}} \cdot \hat{m}_i$ with

$$\vec{B}_{\mathrm{eff}} = J_{\mathrm{IEC}} \hat{m}_R / \mu. \quad (2)$$

Thereby, in the case of out-of-plane anisotropy, $\vec{B}_{\mathrm{eff}}$ always points either parallel or antiparallel to the multilayer depending on the sign of J_{IEC}. J_{IEC} is determined from first principles as half of the total-energy difference between the parallel and antiparallel orientation of the magnetic moments of the free and reference layers.

We apply this model to the prototype system Mn/W(001) with parameters including the Heisenberg exchange up to seventh neighbor shells, the nearest-neighbor DMI, and uniaxial anisotropy, all obtained from first principles [24]. We estimated the contribution of the dipole-dipole interactions and found the contribution negligibly small with respect to other energy terms [24]. We confirm an atomic-scale chiral SS ground state in excellent agreement with experiment [18].

We have minimized the Hamiltonian (1) considering two equivalent limiting cases $B_{\mathrm{app}} = 0$ and $J_{\mathrm{IEC}} = 0$. We have identified the critical fields B_{tr1} and B_{tr2} and the corresponding IEC for the transition between the SS, hexagonal Skyrmion lattice (SkL), and saturated ferromagnetic (FM) states, see Fig. 1(c). To emphasize the equivalence of the two limiting cases, the values of both B_{app} and J_{IEC} are given in the bottom and top axes in Fig. 1(c), respectively. The lower panel shows the equilibrium magnetization accompanied by the jumps at corresponding phase transitions. The inset shows the equilibrium period lengths of the SS (P_{SS}) and the hexagonal SkL (P_{SkL}) and the diameter (D_{iSk}) of an iSk. Obviously, we expect atomic-scale Skyrmions with a diameter of 2–3 nm.

Figure 1(c) illustrates the significant difference between the SkL and the iSk. In contrast to the SkL, which may appear as a metastable state at a zero magnetic field, the iSk at low field exhibits an elliptical instability at B_{iSkE} and does not exist for fields below B_{iSkE}. Moreover, the iSk shows remarkable size variations in strong contrast to the

small changes in the period length of the SkL. Note that in the case of very strong uniaxial anisotropy the metastable iSk can be stabilized at a zero applied field [16]. However, the size of such Skyrmions and the required values of the anisotropy became unrealistic, for details see Ref. [24].

To illustrate the temperature dependence of the critical fields and the corresponding IEC, using Monte Carlo simulations we have calculated the magnetic phase diagram presented in Fig. 1(d) and also in Ref. [24]. This phase diagram describes the general behavior of two-dimensional chiral magnets and is in a good qualitative agreement with experimental observations [9,10] as well as with the recently reported results of Monte Carlo simulations for Pd/Fe/Ir [40]. The phase transition lines between the SS and the SkL as well as between the SkL and the FM states exhibit only a weak temperature dependence and therefore the applied magnetic field or the IEC required to stabilize the SkL remains the same even at high temperatures. On the other hand, the range of existence for the iSk strongly depends on temperature. We have found a critical temperature T_c^* above which the average energy of the thermal fluctuations becomes higher than the energy barrier that protects the iSk from collapse. In this particular case of Mn/W(001), T_c^* is found to be approximately half the ordering temperature $T_c \approx 110$ K, but in general, it is a function of material parameters and may vary for different systems. In a certain region above T_c^*, marked as the yellow area in the phase diagram, spontaneous annihilation and nucleation of the iSk take place. We refer to this state as the boiling Skyrmion soup, because the Skyrmions appear and disappear as bubbles on the surface of the boiling water. The physical reason for the appearance of the Skyrmion soup is that the energy barriers for the transition between the iSk and FM state, ΔE_{SkF}, as well as the reverse one ΔE_{FSk}, become comparable to the energy of thermal fluctuations $k_B T$, see the inset in the phase diagram. The Skyrmion soup state also can be interpreted as the special B-T range where the saturated ferromagnetic ground state becomes unstable with respect to spontaneous nucleation and following the annihilation of the Skyrmions. Experimental measurements of the Skyrmion lifetime in this state provide direct access to the estimation of the energy barriers controlling the Skyrmion nucleation and annihilation processes. As far as the stability range of the iSk is temperature dependent, it is important to identify the optimal magnetic field for which the iSk remains stable within the whole range of temperature between 0 K and T_c^*.

According to the phase diagram, both the iSk and SkL phases are stable over a large range of magnetic fields and temperature. The optimal field to stabilize the iSk has to be fixed slightly above B_{tr2}. For the SkL, this field has to be between B_{tr1} and B_{tr2}; both can be experimentally identified from the jumps on the magnetization curve, Fig. 1(c). For the prototype system Mn/W(001) discussed in this Letter, we indeed find magnetic fields with gigantic values, $B_{\mathrm{tr1}} \approx 18$ T and $B_{\mathrm{tr2}} \approx 37$ T.

In order to realize the appropriate field B_{eff} in terms of the IEC field [Eq. (2)] exerted on the Mn free layer of the Mn/W(001) system, we devised a realistic multilayer system $\mathrm{Mn/W}_m/\mathrm{Co}_n/\mathrm{W(001)}$ and estimated the number of atomic layers m and n by *ab initio* calculations to design a reference layer that fulfills conditions (i)–(iii) mentioned above. For the case of $n = 1$, the results of the IEC between Mn and Co and the magnetic anisotropy of Co as a function of the number of W spacer layers m are presented in Figs. 2(a) and 2(b), respectively. The IEC in Fig. 2(a) exhibits an oscillatory behavior and for $m \leq 7$ the corresponding effective field varies in the range of a few tens of teslas. For the spacer thicknesses $m = 5, 6$, and 7, the effective magnetic fields are about 60, 25, and 21 T, respectively, which are inside the range of magnetic fields required for Skyrmion stabilization, see Figs. 1(c) and 1(d). The thickness of the nonmagnetic spacer affects also the magnetocrystalline anisotropy (MCA) energy, Fig. 2(b). The magnetic moments of about $\mu_{\mathrm{Mn}} = 3.1\ \mu_B$ and $\mu_{\mathrm{Co}} = 1\ \mu_B$ on Mn and Co, respectively, depend only weakly on m (not shown).

Another important parameter that needs to be examined is the exchange stiffness of the Co layer, which has to be large enough to realize a hard FM reference layer. In Table I, we present the *ab inito* results for multilayer systems of different Co thicknesses and interfaces for a given W spacer layer.

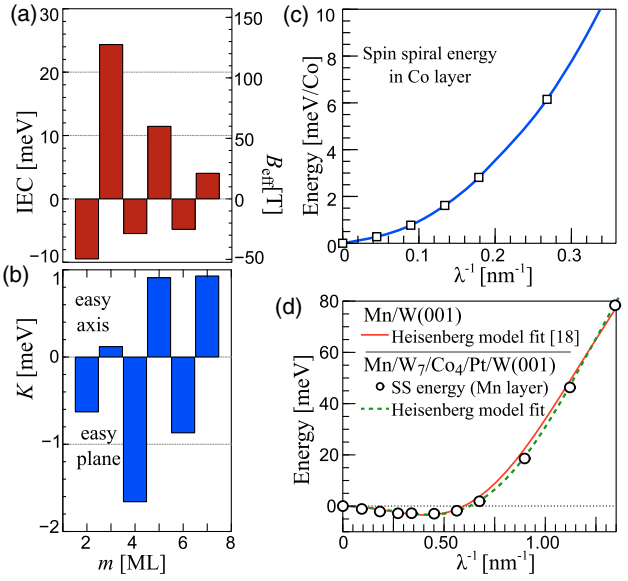

FIG. 2. (a) Strength of the IEC between Mn and Co and (b) the MCA of the Co monolayer with respect to the thickness m of the W spacer, corresponding to the calculation for $\mathrm{Mn/W}_m/\mathrm{Co}_n/\mathrm{W(001)}$ with $n = 1$. For $\mathrm{Mn/W_7/Co_4/Pt/W(001)}$, panels (c) and (d) represent the energy of a flat homogeneous SS for the reference Co (squares) and the free Mn (circles) layers, respectively, calculated without SOC with respect to the inverse SS period length λ^{-1} along the $\langle 110 \rangle$ direction. The dashed (green) line is the fit to the Heisenberg model to calculate the exchange parameters. The solid (red) line is a fit to the Heisenberg model for the pristine Mn/W(001) system, used for the calculation presented in Fig. 1.

TABLE I. Results of *ab initio* calculations for multilayers of different geometry, $Mn/W_7/Co_n/Pt/W(001)$. Magnetic moment of Co μ_{Co} as well as the energy of FM stability $\Delta\epsilon$ and the MCA energy $\tilde{K}_{Co}$ of the reference layer calculated per magnetic Co atom. In particular, for the last example system, the Co magnetic moment at the W/Co interface is very small compared to other Co atoms and we consider it as a nonmagnetic atom in Eq. (1). $\tilde{K}_{Co} > 0$ refers to the out-of-plane easy axis.

Multilayer system	Magnetic moment of Co (μ_B)	$\Delta\epsilon$ (meV)	$\tilde{K}_{Co}$ (meV)
$Mn/W_7/Co_1/W(001)$	1.04	1	0.93
$Mn/W_7/Co_3/W(001)$	0.52, 1.29, 0.29	15	−0.05
$Mn/W_7/Co_3/Pt/W(001)$	0.44, 1.56, 1.68	68	−0.41
$Mn/W_7/Co_4/Pt/W(001)$	0.15, 1.57, 1.72, 1.62	135	1.12

The energy difference $\Delta\epsilon > 0$ represents the stability energy of the FM state of Co calculated with respect to the antiferromagnetic $c(2\times 2)$ state, which is known to be the ground state for the Co ML on the W(001) system [42]. The higher value of $\Delta\epsilon$ is attributed to the higher exchange stiffness and $\Delta\epsilon$ increases with the number of Co layers. We have found that the Co/W interface significantly reduces the magnetic moment of the Co atom at the interface and inhibits the hardness of the thin reference layer.

To achieve a high exchange stiffness we modify the Co/W interface by introducing an additional Pt ML. The Co/Pt/W interface shows a strong influence on $\Delta\epsilon$ and μ_{Co}; both are increased significantly compared to the pure Co/W interface (compare rows 2 and 3 in Table I). The thickness and the interface composition also affect the MCA of the Co layer (see the last column in Table I). For the case of four Co MLs, both a strong out-of-plane $\tilde{K}_{Co}$ and a large positive $\Delta\epsilon$ are achieved.

Focusing on the $Co_4/Pt/W(001)$ system, to characterize the $Mn/W_m/Co_4/Pt/W(001)$ system, for $m = 7$, we have calculated from first principles the energy dispersion for homogeneous flat SSs in the reference and free layers, Figs. 2(c) and 2(d). Such a SS is characterized by a wave vector $\mathbf{q}$ or period length $\lambda = 2\pi/|\mathbf{q}|$. Following the approach proposed in Ref. [43], from fits to the energy dispersion we extracted the parameters $\tilde{A}_{Co} = A/V_{Co}$, $\tilde{D}_{Co} = D/V_{Co}$, and $\tilde{K}_{Co} = K/V_{Co}$ where A, D, and K are the micromagnetic constants of the exchange stiffness, DMI, and uniaxial anisotropy, respectively, and V_{Co} is the average volume per single Co atom in the unit cell. The interplay between these three quantities determines the magnetic ground state of a system. The criterion for the stability of the homogeneous FM state is $\kappa = \pi D/(4\sqrt{AK}) < 1$ [44].

An exchange stiffness constant of $\tilde{A}_{Co} = 90$ meV · nm^2 and an average DMI constant of $\tilde{D}_{Co} = -1.62$ meV · nm are calculated from the energy dispersion without and with SOC, respectively (for details see Ref. [24]). Note that both the interfaces W/Co (−1.9 meV·nm) and Co/Pt (−2.7 meV·nm) contribute to the average $\tilde{D}_{Co}$. We estimate the average out-of-plane anisotropy of the Co layer to be $\tilde{K}_{Co} = 1.12$ meV.

Taking into account the values of $\tilde{A}_{Co}$, $\tilde{D}_{Co}$, and $\tilde{K}_{Co}$ and their ratios to the corresponding micromagnetic constants, we have estimated $\kappa = 0.13$, which shows that the assumption of a hard FM reference layer with out-of-plane anisotropy as required in our model is fully satisfied for the prototype system of $Mn/W_7/Co_4/Pt/W(001)$.

Finally, we examine the influence of the underlying Co reference layer on the coupling parameters of the Mn free layer. From the *ab initio* calculations for $Mn/W_7/Co_4/Pt/W(001)$ we have estimated the coupling constants for the Heisenberg exchange as the dominant energy term. In Fig. 2(d), the energy dispersion of the flat SS in the Mn layer is shown. One can see a behavior equivalent to the pristine $Mn/W(001)$ system. A fit to the Heisenberg model reveals that the exchange interactions J_{ij} remain almost unchanged, see Ref. [24]. The DMI, which is the sum of the layer resolved contributions of the first few layers [43], remains unchanged for a nonmagnetic spacer thick enough, $m \geq 5$. For $Mn/W_7/Co_4/Pt/W(001)$, we have found an about 56% higher out-of-plane MCA, $\tilde{K}_{Mn} = 5.6$ meV, for the Mn layer as compared to the pristine $Mn/W(001)$, 3.6 meV.

Summarizing all the results for the $Mn/W_m/Co_n/Pt/W(001)$ multilayer system, we conclude that the multilayers engineered with $m = 5$ and $m = 6$ W spacer layers and with a reference layer of $n = 4$ Co layers are the best candidates for stabilizing the iSk and the SkL, respectively, without an applied magnetic field. In the systems with $m = 5$, 6, and 7 layers of W, the IEC exerts huge effective out-of-plane magnetic fields of about 42, 22, and 15 T onto Mn with a strong out-of-plane anisotropy $\tilde{K}_{Co}$ of about 0.95, 0.83, and 1.12 meV/Co atom, respectively. The presence of the reference layer modifies slightly the MCA energies of Mn, $\tilde{K}_{Mn}$, to about 4.4, 4.5, and 5.6 meV, respectively, but this has little influence on the Skyrmion size and on Skyrmion formation.

In conclusion, we extended the micromagnetic concept of stabilizing Skyrmions by applied magnetic fields to Skyrmions stabilized by interlayer exchange coupling. This enables Skyrmion formation in chiral magnets with competing exchange interactions that lead to more complicated magnetic ground states such as exchange spin spirals that result in atomic-scale Skyrmions, which may be robust over wide temperature and magnetic field ranges. Replacing the prototype system $Mn/W(001)$ by the multilayer system $Mn/W_m/Co_n/Pt/W(001)$, we have shown that by varying geometrical parameters such as the thickness and fixed-layer compositions, one can achieve a stabilization of small-scale ($D_{iSk} \approx 2$ nm) magnetic Skyrmions even when the required

applied magnetic field would have been gigantic. Our approach is rather general and can be used for any two-dimensional chiral magnet with a surface or interface induced DMI and thus provides a perspective direction to extend the number of possible systems where magnetic Skyrmions can be observed also at elevated temperatures.

The authors acknowledge assistance by David S. G. Bauer and P. Ferriani in evaluating the parameters entering the model Hamiltonian. The authors thank B. Dupé, B. Zimmermann, S. Heinze, A. Fert, and V. Cros for fruitful discussions and acknowledge M. Hoffmann for a critical reading of the manuscript. The authors acknowledge financial support from the MAGicSky Horizon 2020 European Research FET Open Project No. 665095. Computations were performed under the auspices of the Jülich Supercomputing Centre of the Forschungszentrum Jülich.

*a.nandy@fz-juelich.de

[1] I. Dzyaloshinskii, J. Phys. Chem. Solids **4**, 241 (1958).
[2] T. Moriya, Phys. Rev. **120**, 91 (1960).
[3] A. Fert, V. Cros, and J. Sampaio, Nat. Nanotechnol. **8**, 152 (2013).
[4] N. S. Kiselev, A. N. Bogdanov, R. Schäfer, and U. K. Rößler, J. Phys. D **44**, 392001 (2011).
[5] S. Mühlbauer, B. Binz, F. Jonietz, C. Pfleiderer, A. Rosch, A. Neubauer, R. Georgii, and P. Böni, Science **323**, 915 (2009).
[6] H. Wilhelm, M. Baenitz, M. Schmidt, U. K. Rößler, A. A. Leonov, and A. N. Bogdanov, Phys. Rev. Lett. **107**, 127203 (2011).
[7] W. Münzer, A. Neubauer, T. Adams, S. Mühlbauer, C. Franz, F. Jonietz, R. Georgii, P. Böni, B. Pedersen, M. Schmidt, A. Rosch, and C. Pfleiderer, Phys. Rev. B **81**, 041203(R) (2010).
[8] A. Tonomura, X. Yu, K. Yanagisawa, T. Matsuda, Y. Onose, N. Kanazawa, H. S. Park, and Y. Tokura, Nano Lett. **12**, 1673 (2012).
[9] X. Z. Yu, N. Kanazawa, Y. Onose, K. Kimoto, W. Z. Zhang, S. Ishiwata, Y. Matsui, and Y. Tokura, Nat. Mater. **10**, 106 (2011).
[10] X. Z. Yu, Y. Onose, N. Kanazawa, J. H. Park, J. H. Han, Y. Matsui, N. Nagaosa, and Y. Tokura, Nature (London) **465**, 901 (2010).
[11] S. Heinze, K. von Bergmann, M. Menzel, J. Brede, A. Kubetzka, R. Wiesendanger, G. Bihlmayer, and S. Blügel, Nat. Phys. **7**, 713 (2011).
[12] N. Romming, C. Hanneken, M. Menzel, J. E. Bickel, B. Wolter, K. von Bergmann, A. Kubetzka, and R. Wiesendanger, Science **341**, 636 (2013).
[13] B. Dupé, M. Hoffmann, C. Paillard, and S. Heinze, Nat. Commun. **5**, 4030 (2014).
[14] G. Chen, T. Ma, A. T. N'Diaye, H. Kwon, C. Won, Y. Wu, and A. K. Schmid, Nat. Commun. **4**, 2671 (2013).
[15] B. Dupé, G. Bihlmayer, S. Blügel, and S. Heinze, arXiv: 1503.08098.
[16] A. Bogdanov and A. Hubert, J. Magn. Magn. Mater. **138**, 255 (1994); **195**, 182 (1999).
[17] C. Melcher, Proc. R. Soc. A **470**, 20140394 (2014).
[18] P. Ferriani, K. von Bergmann, E. Y. Vedmedenko, S. Heinze, M. Bode, M. Heide, G. Bihlmayer, S. Blügel, and R. Wiesendanger, Phys. Rev. Lett. **101**, 027201 (2008); **102**, 019901(E) (2009).
[19] P. Grünberg, R. Schreiber, Y. Pang, M. B. Brodsky, and H. Sowers, Phys. Rev. Lett. **57**, 2442 (1986).
[20] S. S. P. Parkin, N. More, and K. P. Roche, Phys. Rev. Lett. **64**, 2304 (1990).
[21] P. Bruno and C. Chappert, Phys. Rev. Lett. **67**, 1602 (1991); **67**, 2592 (1991); Phys. Rev. B **46**, 261 (1992).
[22] P. Bruno, Phys. Rev. B **52**, 411 (1995).
[23] M. Bode, M. Heide, K. von Bergmann, P. Ferriani, S. Heinze, G. Bihlmayer, A. Kubetzka, O. Pietzsch, S. Blügel, and R. Wiesendanger, Nature (London) **447**, 190 (2007).
[24] See Supplemental Material at http://link.aps.org/supplemental/10.1103/PhysRevLett.116.177202, which includes Refs. [18,25–41], for computational and methodological details concerning the electronic structure and Monte Carlo calculations, the determination of the parameters entering the Hamiltonian, the role of the dipole-dipole interaction, the topological charge on a discrete lattice, and additional discussions about the B-T phase diagram and the zero field isolated Skyrmion stabilized by the anisotropy.
[25] http://www.flapw.de.
[26] E. Wimmer, H. Krakauer, M. Weinert, and A. J. Freeman, Phys. Rev. B **24**, 864 (1981).
[27] H. Krakauer, M. Posternak, and A. J. Freeman, Phys. Rev. B **19**, 1706 (1979).
[28] J. P. Perdew, K. Burke, and M. Ernzerhof, Phys. Rev. Lett. **77**, 3865 (1996).
[29] J. P. Perdew and A. Zunger, Phys. Rev. B **23**, 5048 (1981).
[30] L. Udvardi, A. Antal, L. Szunyogh, Á. Buruzs, and P. Weinberger, Physica (Amsterdam) **403B**, 402 (2008).
[31] J. M. Borwein and P. B. Borwein, *Pi and the AGM: A Study in Analytic Number Theory and Computational Complexity* (John Wiley & Sons, Inc., New York, 1987).
[32] A. Fert and P. M. Levy, Phys. Rev. Lett. **44**, 1538 (1980).
[33] Mathematica, Version 10.4 (Wolfram Research, Inc., Champaign, IL, 2016).
[34] P. D. Landau and K. Binder, *A Guide to Monte Carlo Methods in Statistical Physics*, (Cambridge University Press, Cambridge, England, 2000).
[35] P. J. van Laarhoven and E. H. Aarts, *Simulated Annealing: Theory and Applications*, (D. Reidel, Dordrecht, Holland, 1987).
[36] C. H. Bennett, J. Comput. Phys. **22**, 245 (1976).
[37] D. Hinzke and U. Nowak, Comput. Phys. Commun. **121–122**, 334 (1999).
[38] B. Berg and M. Lüscher, Nucl. Phys. **B190**, 412 (1981).
[39] M. Janoschek, M. Garst, A. Bauer, P. Krautscheid, R. Georgii, P. Böni, and C. Pfleiderer, Phys. Rev. B **87**, 134407 (2013).
[40] L. Rózsa, E. Simon, K. Palotás, L. Udvardi, and L. Szunyogh, Phys. Rev. B **93**, 024417 (2016).
[41] A. Bogdanov and A. Hubert, Phys. Status Solidi B **186**, 527 (1994).
[42] P. Ferriani, S. Heinze, G. Bihlmayer, and S. Blügel, Phys. Rev. B **72**, 024452 (2005).
[43] B. Zimmermann, M. Heide, G. Bihlmayer, and S. Blügel, Phys. Rev. B **90**, 115427 (2014).
[44] I. E. Dzyaloshinskii, Sov. Phys. JETP **20**, 665 (1965).